



Glacial lake outburst flood hazard under current and future conditions: first insights from a transboundary Himalayan basin

Simon K. Allen^{1,2}, Ashim Sattar¹, Owen King³, Guoqing Zhang^{4,5}, Atanu Bhattacharya^{3,6}, Tandong
5 Yao^{4,5}, Tobias Bolch³

¹Department of Geography, University of Zurich, Zurich, CH-8057, Switzerland

²Institute for Environmental Science, University of Geneva, CH-1205, Geneva

³School of Geography and Sustainable Development, University of St Andrews, St Andrews, KY16 9AL, UK

10 ⁴Key Laboratory of Tibetan Environmental Changes and Land Surface Processes, Institute of Tibetan Plateau Research, Chinese Academy of Sciences (CAS), Beijing, China

⁵CAS Center for Excellence in Tibetan Plateau Earth Sciences, Beijing, China

⁶Department of Remote Sensing & GIS, JIS University, Kolkata 700109, India

Correspondence to: Simon K. Allen (skallenz@gmail.com)



15 Abstract

Glacial lake outburst floods (GLOFs) are a major concern throughout High Mountain Asia, where impacts can be far-reaching. This is particularly true for transboundary Himalayan basins, where risks are expected to further increase as new lakes develop. Given the need for anticipatory approaches to disaster risk reduction, this study aims to demonstrate how the threat from a future lake can be feasibly assessed along-side that of current lakes, and how this information can feed practically into decision-making and response planning. We have focused on two well-known dangerous lakes (Galongco and Jialongco), comparing the consequences of simulated worst-case outburst events from these lakes both in the Tibetan town of Nyalam and downstream at the border with Nepal. In addition, a future scenario has been assessed, whereby an outburst was simulated for a potential new lake forming upstream of Nyalam. Results show that although smallest in size, Jialongco, poses the greatest immediate threat to Nyalam and downstream communities, owing to the high potential for an ice avalanche to trigger an outburst. The future lake scenario would lead to flow depths and velocities that exceed either of the current scenarios, and the peak flood would reach Nepal up to 20 minutes faster. Based on these findings, a comprehensive approach to disaster risk reduction is called for, combining early warning systems with effective land use zoning and capacity building programs. Such approaches address the current drivers of GLOF risk in the basin, while remaining robust in the face of future emerging threats.

30 Keywords

Glacial lake outburst flood, hazard, risk, future, Himalaya

1 Introduction

Widespread retreat of glaciers has accelerated over recent decades in the Himalaya as most other mountain regions worldwide as a consequence of global warming ((Bolch *et al.*, 2019; King *et al.*, 2019; Maurer *et al.*, 2019; Zemp *et al.*, 2019). A main consequence has been the rapid expansion and new formation of glacial lakes (Gardelle *et al.*, 2011; Nie *et al.*, 2017; Shugar *et al.*, 2020), which has large implications for both water resources and hazards (Haeberli *et al.*, 2016a). When water is suddenly and catastrophically released, Glacial Lake Outburst Floods (GLOFs) can devastate lives and livelihoods up to hundreds of kilometres downstream (Carrivick and Tweed, 2016; Lliboutry *et al.*, 1977). This threat is most apparent in the Himalaya, where glacial lakes have been increasing rapidly in both size and number (Gardelle *et al.*, 2011; Zhang *et al.*, 2015), and where a high frequency of GLOFs have been recorded (Harrison *et al.*, 2018; Nie *et al.*, 2018; Veh *et al.*, 2019). The fact that GLOFs can extend across national boundaries exacerbates the challenges for early warning or other risk reduction strategies, particularly in politically sensitive regions (Allen *et al.*, 2019; Khanal *et al.*, 2015a).

Lakes can develop either underneath (subglacial), at the side, in front (proglacial), within (englacial), or on the surface of a glacier (supraglacial), with the dam being composed of ice, moraine or bedrock. Most scientific attention has focussed upon the hazard associated with the catastrophic failure of moraine dammed lakes, and particularly those trapped behind proglacial moraines (e.g., Fujita *et al.*, 2013; Westoby *et al.*, 2014; Worni *et al.*, 2012). Such lakes can be very large, with volumes of up to 100 million m³, and depths exceeding 200 m (Cook and Quincey, 2015), and are susceptible to a range of failure mechanisms owing to the low material strength of the dam structure (Clague and Evans, 2000; Korup and Tweed, 2007). In Asia, as elsewhere in the world, displacement waves generated from large impacts of ice or rock have contributed to the majority of moraine dam failures, occurring predominantly over the warm summer months (Emmer and Cochachin, 2013; Liu *et al.*, 2013; Richardson and Reynolds, 2000). GLOFs have proven particularly common in Tibet, with at least 17 GLOF disasters (causing loss of life or infrastructure) documented since 1935, mostly originating in the central-eastern section of the Himalaya (Nie *et al.*, 2018). Coupled with rapidly increasing population and infrastructural development in the region, an urgent need for



55 authorities to take action and implement timely risk reduction measures has been acknowledged (Wang and Zhou, 2017),
 considering the best available knowledge on existing threats (e.g., Allen *et al.*, 2019; Wang *et al.*, 2015a, 2018), but also with
 a view to the future (Furian *et al.*, 2021; Zheng *et al.*, 2021a).

60 Despite no clear trend observed in GLOF activity over recent decades in the Himalaya (Veh *et al.*, 2019), the ongoing
 expansion of lakes towards steep and potentially destabilised mountain flanks is expected to lead to new challenges in the
 future with implications for hazards and risk (Haeberli *et al.*, 2016b). Based on approaches to model the possible future
 expansion and development of new lakes (Linsbauer *et al.*, 2016) several studies have aimed to quantify the possible
 implications for GLOF frequency and/or magnitude for different regions (Allen *et al.*, 2016; Emmer *et al.*, 2020; Magnin
 65 *et al.*, 2020). For example, in the Indian Himalayan state of Himachal Pradesh, Allen *et al.* (2016) demonstrated a 7-fold increase
 in the probability of GLOF triggering and a 3-fold increase in the downstream area affected by potential GLOF paths under
 future deglaciated conditions. Meanwhile, Zheng *et al.* (2021a) have elaborated such analyses for the entire High Mountain
 Asia, revealing an almost 3-fold increase in GLOF risk and the emergence of new hotspots of risk over the course of the 21st
 century. Significantly, the number of lakes posing a transboundary threat within border areas of China and Nepal could double
 70 in the future, particularly within the eastern Himalayan region (Zheng *et al.*, 2021a). While such large-scale, first-order studies
 are important for raising general awareness of the future challenges that mountain regions will face (Hock *et al.*, 2019), there
 are limitations in the extent to which these studies can directly inform planning and response actions at the ground level.

The need for forward-looking, anticipatory approaches to hazard and risk modelling is clearly recognised within recent
 international guidelines on glacier and permafrost hazard assessment (GAPHAZ, 2017), yet practical examples on how to
 75 integrate future lake development for GLOF assessment and risk management are lacking. International best practice is framed
 by both a first-order assessment undertaken at large scales (to identify potentially critical lakes), followed by a detailed
 assessment for these lakes using numerical models to simulate downstream flood intensities as a basis for hazard mapping
 (GAPHAZ, 2017). This is a common approach for existing threats, where the time, data, and expertise needed to invest in
 comprehensive hazard modelling and mapping can be well justified for a lake that is determined to be critical. However, for
 80 future lakes, where the formation of the lake and its eventual dam characteristics remain highly uncertain, there remains a
 methodological gap in the hazard assessment process, as authorities are unlikely to undertake sophisticated hazard mapping
 for a threat that may not even eventuate. In this study we aim to address this gap, by providing an illustrative example of how
 the threat of a potential future lake can be feasibly assessed along-side that of current lakes, and how this information can feed
 practically into decision-making and response planning in a transboundary context.

85 Focusing on the transboundary Poiqu river basin in the central Himalaya, the specific objectives of the study are to 1) apply
 hydrodynamic modelling and systematic criteria to assess the magnitude and likelihood of worst-case outburst events from
 two potentially critical lakes in the Poiqu river basin, 2) compare the results with a potential outburst from a large lake that is
 anticipated to develop in the future, and 3) discuss the implications for early warning or other risk reduction strategies. This
 90 study is intended to provide timely input to the scoping and design phase of future GLOF risk reduction strategies in the Poiqu
 basin, to ensure early warning systems and other measures remain suitable under possible future scenarios.

2 Study area

This analyses focuses on a ca. 40 km stretch of the lower Poiqu river basin originating from Galongco glacial lake, considering
 GLOF impacts in Nyalam town (capital of Nyalam county, Tibetan Autonomous Region), and downstream to the border with



95 Nepal at Zhangmu (Fig. 1). The elevation range of the study area extends over 6000 metres, from the summit of Shishapangma
 at 8,027 m a.s.l, whose glacierised slopes feed Galongco, to 2000 m a.s.l in the river valley at Zhangmu. According to Wang
 and Jiao (2015), mean annual temperature and mean annual precipitation in Nyalam (3810 m asl) are 3.8°C and 650.3 mm
 respectively, with sub-zero temperatures lasting from November – March each year. Temperatures peak in July (10.8°C), while
 highest precipitation rates are recorded in September (87.9 mm/month). In total, 60% of the annual rainfall falls during the
 100 monsoon months of July – September (Wang *et al.*, 2015b)

The Poiqu basin is the Tibetan portion of the large transboundary Poiqu/Bhote Koshi/Sun Koshi River Basin, along which the
 economically important Friendship Highway links China to Nepal, and where significant hydropower resources are located
 (Khanal *et al.*, 2015b). Based on a larger study across Tibet, the Poiqu basin has been identified as a clear hotspot of
 105 transboundary GLOF danger (Allen *et al.* 2019 – Fig. 1), where at least 6 major GLOF events reported over the past century,
 including repetitive events from Jialongco in 2002 (Chen *et al.*, 2013), and Cirenmaco in 1964, 1981 and 1983 (Wang *et al.*,
 2018). The 1981 event resulted in numerous fatalities, and estimated losses of up to US\$4 million as a result of damage to
 houses, roads, hydropower, and disruption to trade and transportation services (Khanal *et al.*, 2015a). Meanwhile an outburst
 of $1.1 \times 10^5 \text{ m}^3$ from Gongbatongshacuo (adjacent to Cirenmaco) in July 2016, resulted in significant damage to hydropower
 110 and roads, exacerbating losses inflicted one year earlier by the Gorka earthquake (Cook *et al.*, 2018). Whereas
 Gongbatongshacuo has completely drained, Cirenmaco remains a large and persistent threat, considered as one of the most
 dangerous lakes in Tibet (Allen *et al.*, 2019; Wang *et al.*, 2018).

In the current study, we focus not on Cirenmaco, which has already been the subject of comprehensive investigations (Wang
 115 *et al.*, 2018), but rather on two other well documented threats of Jialongco and Galongco, owing to their potential to cause
 damage to the Tibetan county capital of Nyalam, and downstream in Nepal. Both lakes have expanded rapidly over the past
 decades, with Galongco, the largest lake in the basin, increasing its area by 450% from 1.00 to 5.46 km² in the period 1964-
 2017 (Wang *et al.*, 2015b; Zhang *et al.*, 2019).

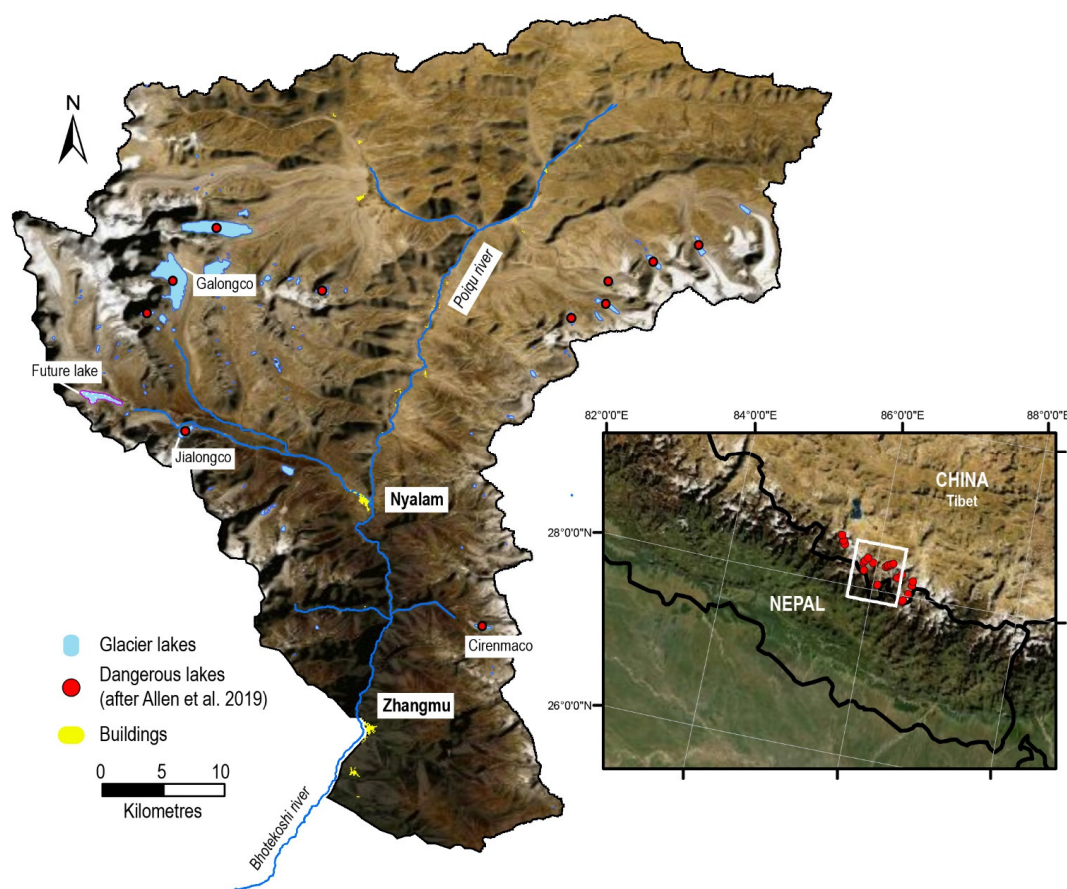


Figure 1: Location of the Poiqu River basin within a hotspot of GLOF risk, as determined on the basis of 30 potentially most dangerous lakes identified across Tibet (after Allen et al. 2019). The current lakes focussed on in this study of Galongco and Jialongco are indicated, as is the modelled future lake, the county capital town of Nyalam, and border town of Zhangmu. Cirenmaco, from which several outburst floods have been reported, is also indicated; Background image: ESRI Basemap Imagery.

3 Methodological approach

In line with recent international guidance in GLOF hazard assessment (GAPHAZ 2017), in this study we consider lake susceptibility, which determines the likelihood of a given outburst scenario to occur, and use hydrodynamic modelling to determine downstream impacts. In order to compare the threat posed by the two current lakes with a future anticipated lake, we focus on worst-case scenario modelling – that is to say, the maximum outburst volume that could be produced from Jialongco, Galongco, and the anticipated future lake.

3.1 GLOF Modelling

The total volume of water potentially released during a GLOF event is of critical importance for hydrodynamic modeling of a GLOF scenario (Westoby *et al.*, 2014). In this study, the volumes for Jialongco and Galongco were estimated by multiplying



mapped lake area (A) by estimated mean depth (D_m), where D_m is calculated according to the empirical relationship of Fujita et al. (2013) which has been established based on lake data from the Himalayan region:

$$D_m = 55A^{0.25} \quad (1)$$

where A and D_m are the lake area (km^2) and mean depth (m). Lake area was mapped using Google Earth imagery from 2019. For GLOF modelling of the future lake, the location and maximum volume of the potential lake upstream from Jialongco is based on a modelled overdeepening in the glacier bed topography using GlabTop (Linsbauer et al., 2012). The model is now well established for providing a first-order indication of where lakes may develop in the future (e.g., Allen et al., 2016; Haeberli et al., 2016a; Linsbauer et al., 2016; Magnin et al., 2020). The ice thickness distribution from GlabTop is subtracted from a surface DEM to obtain the bed topography, i.e. a DEM without glaciers, from which overdeepenings in the glacier bed can be detected and volumes estimated. Inputs to the model include manually edited glacier branch lines, and a DEM – in this case the NASA Shuttle Radar Topography Mission (SRTM) Version 3.0 (void filled) was used, at 30 m resolution. While the model predicts several possible locations in the Poiqu basin where large future lakes can develop, we focussed on the largest of these lakes that threaten the town of Nyalam. Beyond its potential size, this overdeepening was selected owing to its position in an area of the low surface gradient behind a pronounced terminal moraine, beneath a tongue where supraglacial ponds are already developing, and at an elevation that is lower than other overdeepenings in the area. All factors provide favourable preconditioning for the formation of a large proglacial lake (Frey et al., 2010; Linsbauer et al., 2016)

Based on the total estimated volume of the lakes, we then establish the potential flood volume (PFV) for each lake following the concept of Fujita et al. (2013), that assumes full incision and removal of the downstream slope of the dam (Fig 2a). Only where the height of the potential breach (h_b) is greater than the mean depth of the lake is the full release of the lake volume possible:

$$\text{PFV} = \min[h_b; D_m]A \quad (2)$$

For example, in the case of Jialongco, the breach height is estimated at 40 m, which is less than the mean depth of the lake suggesting that even following full moraine incision, some water will remain in the lake (Fig 2b). The resulting PFV is therefore estimated at $24.8 \text{ m}^3 \cdot 10^6$ ($40 \text{ m} \times 0.62 \text{ km}^2$). In comparison, the well documented 1981 outburst from the smaller Cirenmaco was estimated to have involved a breach height of up to 60 m and an outburst volume of $19 \text{ m}^3 \cdot 10^6$ (Xu, 1988). In principle, dam geometries can be measured directly in Google Earth, although there can be severe distortions in the imagery in some regions and the DEM accuracy is unknown. Therefore, to achieve a higher level of accuracy, we measured h_b and other topographic parameters using spot elevations extracted from a higher resolution (1 m grid cell) Digital Elevation Model, generated from 0.5 m resolution tri-stereo Pleiades imagery acquired in October 2018, covering the whole Poiqu basin (Bhattacharya et al., 2021).

Subsequent breach parameters were calculated according to Froehlich (1995) for each outburst scenario:

$$B_w = 0.1803K_o (V_w)^{0.32} (h_b)^{0.19} \quad (3)$$

$$T_f = 0.00254 (V_w)^{0.53} (h_b)^{-0.9} \quad (4)$$

where B_w is the breach width (in m), K_o is a constant which is considered to be 1.4 for overtopping failures, V_w is the volume above h_b of the lake (in m^3), and T_f (in min) is the time taken for the breach to form (where distances B_w and h_b are fully obtained).



The HEC-RAS (v 5.0.7) dam-break module was used to set up different breach scenarios for the three lakes (Table 1). Dam-break simulations were performed where the frontal moraine (dam) is defined to fail, given the calculated breach parameters (after Froehlich, 1995). Here, a progressive breach mechanism was assumed for all the scenarios where overtopping failure initiated at the crest of the moraine spreading downwards and sideways. The outputs in the form of outflow hydrographs (discharge vs. time) were then used as boundary conditions for downstream two-dimensional GLOF routing with HEC-RAS (v 5.0.7) as far as Zhangmu (Fig 3). This hydraulic model solves the Full Saint Venant equations two-dimensionally in an unsteady flow. Two-dimensional routing requires accurate terrain information as a primary input. While several freely available DEMs were tested (e.g., ALOS PALSAR at 12.5 m or HMA at 8 m), topographic artefacts led to modelling errors. As such, the 1-m Pleiades DEM was finally used. The limits of the defined computational flow area extend 500 m on either side of the central line of the flow channel. The flow domain was divided into equal grids of 30×30 m to attain numerical stability while performing unsteady flow computation of the breach hydrographs for each scenario individually. Considering the uniformity of land cover and lack of vegetation along the flow channel, a uniform Manning roughness of 0.045 was considered along the flow channel. The total computation time was set to 24 hours such that the modelled flood wave had enough time to propagate downstream even under potential low momentum conditions. The flow hydraulics (i.e. flow depth and flow velocity) were obtained for each inundated pixel. The time series of flow depth and velocity were measured at a point located at the centre of the river channel at Nyalam and Zhangmu.

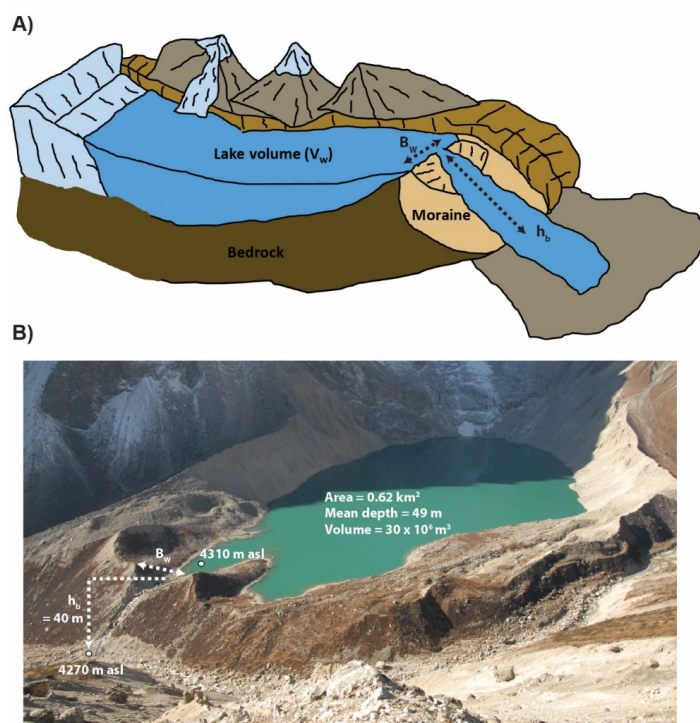


Figure 2: A) Schematic showing key parameters of breach width (B_w) and breach height (h_b). B) Image of Jialongco showing the calculation of breach height, as the difference between the lake surface elevation at the outlet, and elevation at the front of the distal slope of the moraine dam. Photo: O. King (October 2018).



200

3.2 Lake susceptibility assessment

The assessment follows a systematic approach that considers wide-ranging atmospheric, cryospheric and geotechnical factors that can influence lake susceptibility, and thereby the likelihood of a GLOF occurring (after GAPHAZ 2017). As a desk-based assessment, we draw on remotely sensed data to the extent possible, to enable a semi-qualitative comparison of susceptibility factors across the three lakes. Factors assessed, their primary attributes, and sources used are provided in Table 2. Topographic characteristics (dam geometry, slope angles etc) were precisely measured using the high resolution 1m DEM generated from Pleiades imagery. To establish the potential for ice and/or rock avalanche triggering, additional GIS-based analyses were undertaken. The overall likelihood of rock (or debris) avalanches triggering an outburst was calculated based on the concept of topographic potential (Allen *et al.*, 2016; Romstad *et al.*, 2009) which identifies within each lake watershed a) the potential for rock to detach (parameterized by slope angles $>30^\circ$), and b) the potential for the resulting avalanche to reach the glacial lake (parameterized by overall trajectory slopes $>14^\circ$ ($\tan \alpha = 0.25$). Potentially unstable zones of glacial ice were identified in Google Earth, based on orientation and density of crevassing, with a subsequent estimate of the ice thickness and volume provided from the GlabTop model output (Table 3). Furthermore, the time series of Google Earth imagery was examined to identify any evidence of historical mass movements, that could indicate an enhanced threat to the lakes below.

215

3.3 Future lake development

To establish the possibility of lake development and the likely future trajectory of lake area growth on the parent glacier (RGI60-15.09475), we examine the surface velocity, rate of thinning and the evolution of the geometry (surface slope) of the glacier in recent decades. Previous studies (Quincey *et al.*, 2007) have identified glacier surface attributes which may precondition the surface of debris-covered glaciers for supraglacial lake development. Glaciers bounded by large lateral and terminal moraines which have a flat or gently sloping ($<2^\circ$), slowly flowing ($<10 \text{ m a}^{-1}$) main tongue commonly host networks of supraglacial ponds as surface meltwater cannot drain from the glacier surface. Such pond networks expand when the mass balance of the glacier is negative and coalesce to eventually form a supraglacial lake at the hydrological base level of the glacier- the lowest point where the glacier surface intersects the terminal moraine (Benn *et al.*, 2012).

We used the Pleiades DEM and glacier surface elevation change data generated by King *et al.* (2019) to examine the evolution of the geometry of glacier RGI60-15.09475 since the 1970s. Glacier surface slope estimates were derived by the fitting of linear regression models through ‘average’ (mean of 5 evenly spaced) elevation profiles of the glacier surface split into 750 m long segments (King *et al.*, 2018). We also assessed the current flow regime of the glacier using surface velocity data, which was generated through the tracking of glacier surface features visible in Sentinel 2 imagery over the period 2017-2019 (Pronk *et al.*, 2021). Examination of these parameters established that the conditions at the surface of the glacier (Fig. 7) are well suited to imminent glacial lake development considering the factors outlined by Quincey *et al.* (2007).

To investigate the likely size of such a lake in the coming decades we consider two different scenarios of glacier thinning between 2015 and 2100 and follow a similar method to that of Linsbauer *et al.* (2013) to simulate glacier thickness into the future, but employ different criteria to determine future lake area. Our first scenario is based on the assumption that the acceleration in glacier thinning in the Poiqu basin measured by King *et al.* (2019) (Fig. 7) is replicated by the year 2100. Such an increase in thinning will be driven by a further 1°C increase in temperature by 2100 (Kraaijenbrink *et al.*, 2017), further to the $\sim 1^\circ\text{C}$ increase in temperature which has occurred in the central Himalaya (Maurer *et al.*, 2019) since the 1970s. The second scenario is based on the premise that the increase in thinning which has occurred between 1974 and 2015 (Fig. 7) will be replicated over subsequent equivalent time periods (by 2056, 2097, etc). We extrapolated the thinning rates from King *et al.*



(2019) and integrated the resulting elevation changes between 2015 and 2100. We then assumed that once the glacier surface had lowered to a height below the hydrological base level of the glacier (4890 m a.s.l.) meltwater ponding would occur and that DEM pixels with an elevation of less than this threshold represented lake area at that point in time.

4 Results

245 Based on the three assessed lake outburst scenarios, we focus below on results relating to the core hazard dimensions of GLOF magnitude and likelihood (or probability), and assess the exposure of buildings in the town of Nyalam. A full hazard and risk assessment, including a complete range of outburst scenarios and vulnerability mapping, is beyond the scope of this study.

4.1 GLOF impact

250 Worst-case outburst scenarios for the three lakes were simulated until the border between China and Nepal (Zhangmu). Of the two current lakes assessed, the modeled peak discharge from Galongco is more than 14 times larger than that from Jialongo, leading to flow depths up to 5 m higher and velocities up to $2 \text{ m}^3 \text{ s}^{-1}$ faster impacting the town of Nyalam. At the border, 20 km downstream, inundation depths are up to 10 times larger for the Galongco event as the flow becomes constricted in the narrow topography of the valley (Table 1, Fig. 3). A worst-case outburst from the potential future lake, with a release volume of $70 \times 10^6 \text{ m}^3$, and peak discharge of $42,917 \text{ m}^3 \text{ s}^{-1}$, would result in flow depths (20.1 m) and velocities ($13.9 \text{ m}^3 \text{ s}^{-1}$) in Nyalam that would exceed events from both Jialongco and Galongco, while downstream at the border, flow depths would be lower than that of the Galongco outburst (23.8 vs 27.9 m), but with significantly higher velocities (13.9 vs. $9.4 \text{ m}^3 \text{ s}^{-1}$). Differences in failure time, peak velocities, and travel distance, lead to variations in the arrival of the modelled flood waves in Nyalam and further downstream at the border with Nepal, with implications for warning times and response strategies (see Discussion).

260 The flood wave from Jialongco first registers after 48 minutes in Nyalam, with the maximum flow heights arriving 4 minutes later. In contrast, the floodwave from Galongco first registers after 82 minutes, with maximum flow heights arriving 26 minutes later. An outburst from the potential future lake has the quickest arrival time of only 42 minutes in Nyalam, reaching the Nepalese border 30 minutes later (compared to 40 minutes later for the existing lakes).

265 Upstream of Nyalam a backwash effect is produced by the narrowing of the valley, extending for 600 m up the Poiqu river, with maximum flow depths of 25 m. We note that model simulations undertaken using several coarser DEMs (e.g., ALOS PALSAR at 12.5 m or HMA at 8 m) all resulted in significant modelling artefacts in this region immediately up- and downstream from Nyalam owing to voids in the DEMs in this area of complex topography. As a consequence, physically implausible flow depths exceeding 100 m were simulated due to artificial blockages along the river path, while the timing of the floodwave

270 was effected by the stagnation of the flow occurring behind these blockages.

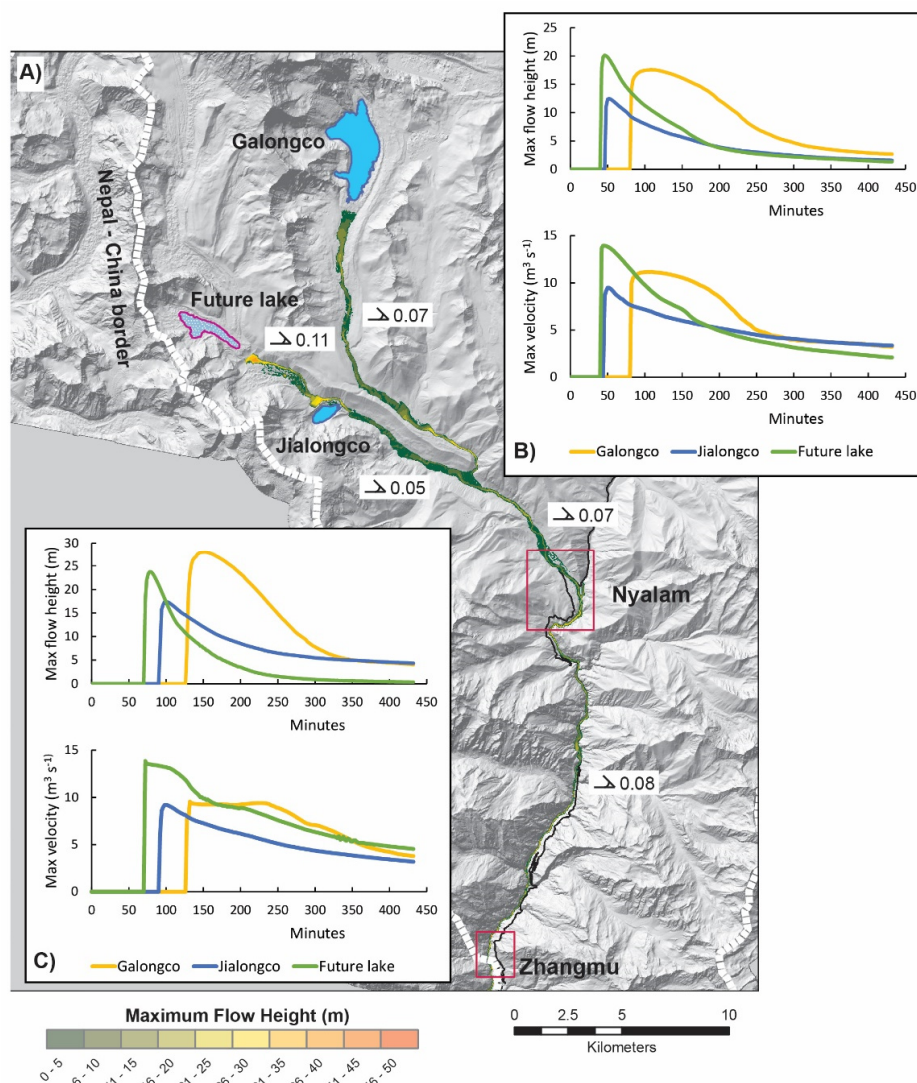
Potential processes that could significantly enhance and/or modify the GLOF magnitude include entrainment of large volumes of sediment along the flow path leading to bulking of the flow volume, blockages of a river by GLOF deposits leading to secondary outburst events, and a process chain involving more than one lake. Significant erosion of sediment and a catastrophic transformation into a debris flow event is considered unlikely for any of the three outburst scenarios, given that average trajectory slope angles measured along the flow paths (Fig. 3) are well below those needed to entrain sediment from within a channel (Huggel *et al.*, 2004). In the absence of significant entrainment of sediment, there is limited potential for large deposits to block adjacent waterways, although erosion and destabilisation of the river banks as a result of the flood waters means that such secondary hazards cannot be excluded, particularly in the steep sided gorge downstream of Nyalam.



Table 1: Measured and modelled lake and outburst flood parameters for the three assessed lakes.

	Galongco	Jialongco	Future lake
Lake area (km ²)	5.46	0.62	1.54
Mean lake depth (m)	84	49	46
Lake volume (10 ⁶ m ³)	459	30	70
Potential flood volume (10 ⁶ m ³)	262	25	70
Breach height (m)	48	40	70
Breach width (m)	260	118	183
GLOF peak (m ³ s ⁻¹)	107,802	7,507	42,917
Time of arrival at Nyalam	82 min	48 min	42 min
Flow depth at Nyalam (m)	17.6	12.5	20.1
Flow velocity at Nyalam (m ³ s ⁻¹)	11.6	9.5	13.9
Time of arrival at Zhangmu	128 min	92 min	72 min
Flow depth at Zhangmu (m)	27.9	17.4	23.8
Flow velocity at Zhangmu (m ³ s ⁻¹)	9.4	9.2	13.9

Results indicate that an outburst event from the potential future lake could slam into, pool up, and eventually overtop the lateral moraine of Jialongco, producing a potential chain reaction where Jialongco also breaches (Fig. 4). Maximum flow heights measured at the surface of Jialongco reach 27 m, suggesting a significant volume of water could enter the lake via overtopping. Simultaneously, the outburst from upstream would lead to erosion at the front distal slope of the Jialongco dam area, as the flow is constrained in this area leading to high energy levels. The combined high-impact low-probability chain reaction involving near-simultaneous breaching of the potential future lake and Jialongco requires more sophisticated modeling to fully analyse downstream impacts, but in a first approximation could lead to maximum combined flow depths >30 m in Nyalam.



290

Figure 3: A) Modelled GLOF flow heights for three assessed lakes. Numbers indicate the overall trajectory slope (tan⁻¹) for different sections along the GLOF paths. Insets B) and C) provide a time series of maximum flow height and maximum velocity measured in Nyalam and downstream at the border town of Zhangmu, respectively.

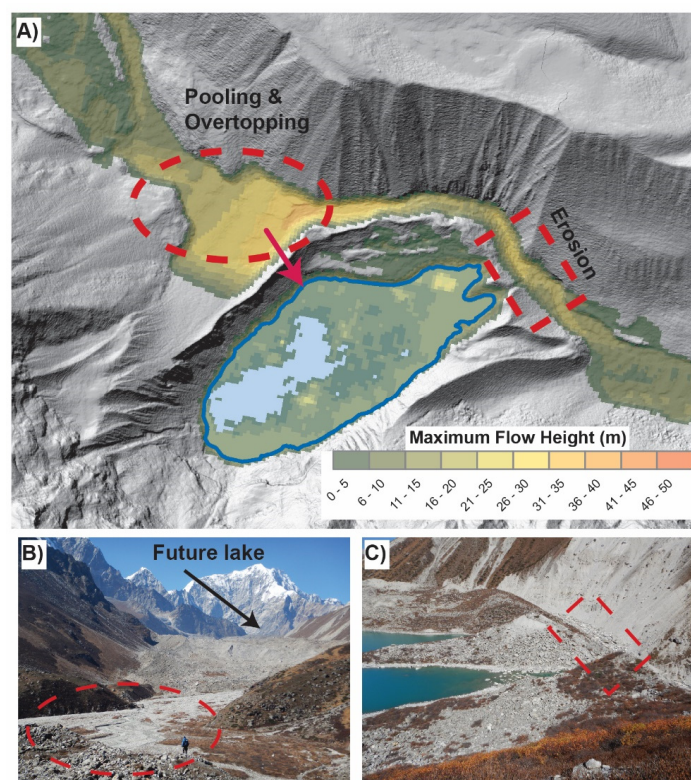


Figure 4: A) Modelled GLOF flow heights for an outburst event from the potential new lake, showing area of pooling and overtopping into Jialongco. Background DEM generated based on Pleiades data 15 Oct 2018 © CNES and Airbus DS. Photos show the area of pooling (B), and flow concentration and potential erosion at the front of Jialongco (C). Photos: S. Allen (October 2017).

4.2 GLOF likelihood

The second component of GLOF hazard concerns the likelihood or probability of an event occurring considering the wide-ranging factors that can condition or trigger an outburst. Taking a systematic approach (after GAPHAZ 2017), we compare the relative susceptibility of the three lakes considered in this study, considering also how this susceptibility might evolve in the future (Table 3). The table distinguishes those factors that condition and/or trigger an outburst event, while also linking to those factors that can influence outburst magnitude (see 4.1). Located in a transitional zone to the north of the main Himalayan divide, the upper Poiqu basin is subject to heavy rainfall during the Asian summer monsoon. With a significantly larger watershed area, Galongco is considered more susceptible to heavy rain and/or snow melt leading to high lake water levels, and under future deglaciated conditions the lake may become fed by a well-developed paraglacial stream network. However, even under these conditions, the relatively favourable dam geometry (low width to height ratio and 15 m dam freeboard) suggests that the likelihood of a catastrophic outburst via this triggering mechanism is low. Similarly, self-destruction via warm temperatures and melting of ground ice within the moraine dam can be effectively discounted. Creeping permafrost features visible in the vicinity of Galongco, and a partially hummocky appearance of the lake dam, suggests some presence of an ice-cored moraine, but the width and gentle downstream slope of the dam would make a catastrophic failure extremely unlikely.



315 As with the majority of large glacial lakes across the Himalaya (Liu *et al.*, 2013; Richardson and Reynolds, 2000; Sattar *et al.*,
 2021), the main triggering threat is considered to come from large slope instabilities, impacting into the lake. Under current
 conditions, Jialongco is considered to be most susceptible to ice avalanches, given the presence of a steep, highly crevassed
 tongue positioned directly behind the lake (Fig. 5). With an average slope of 36° , and large crevasses marking a sharp break
 in topography, full collapse of the glacier tongue ($\sim 20 \times 10^6 \text{ m}^3$) is feasible (Table 4). The mass would impact the lake in a
 320 direction parallel to the longitudinal axis of the lake, leading to maximum overtopping wave heights and swashing effect,
 meaning even a partial collapse of the unstable ice mass could be sufficient to displace the full potential flood volume of the
 lake, irrespective of whether or not the dam is deeply incised. However, further retreat of the tongue will see a reduction in the
 potential avalanche volume, and eventually this threat will be eliminated completely as the ice retreats to a point behind the
 topographic break.

325 In comparison, the largest potential unstable ice masses surrounding Galongco would strike the lake perpendicular to the
 longitudinal axis of the lake (from the west) meaning most of the energy from a displacement wave would be dissipated on the
 opposing side of the lake. Steep ice cliffs located higher on the mountain slopes, including those found currently above where
 the future lake is expected to form, are estimated to have maximum volumes ranging from $0.1 - 1 \times 10^6 \text{ m}^3$ (Table 4), and
 330 therefore are considered insufficient to generate the worst-case outburst flood volumes simulated here. Hence, a large rock or
 combined ice-rock avalanche is considered to be the most feasible mechanism capable of triggering the maximum potential
 outburst flood volume from either Galongco or the potential future lake. A greater likelihood of such an event is identified for
 Galongco, given the sheer size of the catchment meaning greater topographic potential for large rock failures, including from
 the slopes of Shishapangma rising nearly 3000 m above the lake. Similarly, the potential future lake is positioned directly
 335 beneath the $\sim 2000 \text{ m}$ high eastern face of Ramthang Karpo Ri. Given that Poiqu basin is located within a high seismic hazard
 zone (Shedlock *et al.*, 2000), large ice-rock avalanches of the magnitude needed to trigger a worst-case scenario from these
 lakes are possible, but remain extremely rare events. While displacement wave processes depend ultimately on the orientation
 of the incoming mass, and its interaction with lake bathymetry (Schaub *et al.*, 2015), we estimate an avalanche volume in the
 order of 50 million m^3 would be needed to initiate a worst-case outburst from Galongco. This estimate accounts for the
 340 relatively stable dam geometry, requiring a significant amount of the flood volume to be released in the initial overtopping
 wave, which, based on empirical evidence, can be estimated as being up to 10 times the incoming mass (Huggel *et al.*, 2004).
 Even on a global scale, avalanche volumes of this magnitude are extremely rare (Kääb *et al.*, 2021; Schneider *et al.*, 2011),
 making this a high magnitude, but very low likelihood process chain. Finally, all three lakes are susceptible to instantaneous
 or progressive landslides occurring from the adjacent lateral moraines, most notably for Jialongco where active instabilities
 345 are clearly evident. Recent studies have shown that large lateral failures, either instantaneous or progressive, can be sufficient
 to initiate catastrophic process chains where dam geometries are sufficiently prone to erosion (Klimeš *et al.*, 2016; Zheng *et al.*,
 2021b).

Based on the assessment results, a large outburst scenario involving the maximum potential flood volume is considered most
 350 likely under current conditions to originate from Jialongco, triggered by an ice avalanche or large failure of the lateral moraine
 slopes. Large rock or combined ice-rock avalanches are a less likely, but potentially high magnitude trigger of an outburst
 from all 3 lakes considered. Given the large volume of water that would need to be displaced and breach depth that would need
 to occur, the probability of a worst-case scenario originating from Galongco is considered very low. The susceptibility of the
 potential future lake to avalanches, moraine instabilities, or rain and snowmelt, will ultimately depend on the its final dam
 355 geometry, and particularly its freeboard, which is highly uncertain from model results alone.



Table 3: First-order lake assessment of wide-ranging factors determining the susceptibility of glacial lake (based on GAPHAZ 2017). Colours represent an expert assessment of high (orange), moderate (yellow), and low (green) susceptibility for each of the factors considered. No colour indicates the factors were not considered relevant for these lakes. Factors can be relevant for conditioning and/or triggering a GLOF, and can also have an influence on outburst magnitude.

360

Susceptibility factors for GLOFS	Relevance			Relevant Attributes	Susceptibility			Assessment methods and sources
	Con.	Trig.	Mag.		Jialong Co	Galong Co	Future lake	
a) Atmospheric								
Temperature	+	+		Mean temperature	Increasing	Increasing	Increasing	Climate observations and projections (Ren <i>et al.</i> , 2017; Sanjay <i>et al.</i> , 2017)
				Intensity and frequency of extreme temperatures	Increasing	Increasing	Increasing	
Precipitation	+	+	+	Intensity and frequency of extreme precipitation events.	Increasing	Increasing	Increasing	
b) Cryospheric								
Permafrost conditions	+	+		State of permafrost, distribution and persistence within lake dam area and bedrock surrounding slopes	No permafrost in dam. Degrading permafrost in surrounding slopes.	Possible ice-cored moraine dam. Degrading permafrost in surrounding slopes.	No permafrost in dam. Degrading permafrost in surrounding slopes.	Model-based results (Schmid <i>et al.</i> , 2015); Google Earth
Glacier retreat and downwasting	+		+	Enlargement of proglacial lakes, enhanced supraglacial lake formation, dam removal or subsidence	Lake currently at maximum extent. Glacier not in contact with lake.	Minimal potential for further expansion (+1%).	Lake will be actively expanding over several decades, as overdeepening emerges.	GlabTop; Landsat archive (Zhang <i>et al.</i> 2019); Google Earth; DEM differencing (King <i>et al.</i> , 2019)
Advancing glacier (incl. surging)	+			Formation of ice-dammed lakes	Not relevant	Not relevant	Not relevant	Google Earth
Ice avalanche potential		+	+	Steep glacier tongue or ice cliffs, crevasse density and orientation, ice geometry	High potential	Moderate potential	Moderate potential	GlabTop; DEM slope analyses; Google Earth
Calving potential		+	+	Width of glacier calving front, activity, crevasse density	Glacier not in contact with lake.	Minimal potential (calving front = 300 m).	High potential (calving front = > 1km).	Google Earth
Lake size	+		+	Area, volume, and/or depth	Mean depth: 49 m Volume: 30.3 x 10 ⁶ m ³	Mean depth: 84 m Volume: 459 x 10 ⁶ m ³	Mean depth: 61 m Volume: 94 x 10 ⁶ m ³	Landsat-based lake area mapping (Zhang <i>et al.</i> , 2019); Area/depth scaling (Fujita <i>et al.</i> , 2013), GlabTop
c) Geotechnical and Geomorphic								
Dam type	+		+	Bedrock, moraine, ice	Moraine	Moraine	Moraine	Google Earth



Dam width to height ratio	+		+	Width across the dam crest relative to the dam height	4:1	9:1	8:1 (large uncertainty)	Google Earth; High resolution DEM analyses (Pleiades)
Freeboard to dam height ratio	+		+	Elevation difference between lake surface and lowest point of moraine.	~ 20 m	~ 15 m	~ 10 m (large uncertainty)	Google Earth; High resolution DEM analyses (Pleiades)
Downstream slope of dam	+			Mean slope on downstream side of lake dam.	30°	10°	20° (large uncertainty)	Google Earth; High resolution DEM analyses (Pleiades)
Vegetation on dam	+			Density and type of vegetation (grass, shrubs, trees).	Grass/scrub on downstream slope	Absent	Absent	Google Earth
Catchment area	+			Total size of drainage area upstream of catchment	9 km ²	35 km ²	10 km ²	DEM analyses
Catchment mean slope	+			Steepness of catchment area	32°	28°	29°	DEM analyses
Catchment drainage density	+			Density of the stream network in catchment area	Low density stream network to develop under deglaciated conditions.	Moderate density stream network to develop under deglaciated conditions.	Low density stream network to develop under deglaciated conditions.	GIS based hydrological modelling
Catchment stream order	+			Presence of large fluvial streams, facilitating rapid drainage into lake	Low order streams to develop in future	Moderate order streams to develop in future	Low order streams to develop in future	GIS based hydrological modelling
Upstream lakes	+			Presence and susceptibility of upstream lakes.	None currently. Two small lakes (~0.01 km ²) anticipated in future.	None currently or anticipated in future.	None currently or anticipated in future.	GlabTop; Google Earth
Rock avalanche potential		+	+	Steep, structurally unstable bedrock slopes with potential to runoff into the lakes.	TP = 3820 Historical instabilities not evident.	TP = 7760 Historical instabilities not evident.	TP = 3876 Historical instabilities not evident.	GIS-based topographic potential modelling; Google Earth
Moraine instabilities		+	+	Potential for landslides from moraine slopes into the lake	Steep moraine slopes > 500 m high. Large instabilities evident.	Steep moraine slopes 100 – 200 m high. Minor instabilities evident.	Steep moraine slopes in the order of 100 – 200 m anticipated.	Google Earth
Seismicity		+		Potential magnitude & frequency, ground acceleration	High	High	High	Global Seismic Hazard Map (Shedlock <i>et al.</i> , 2000)

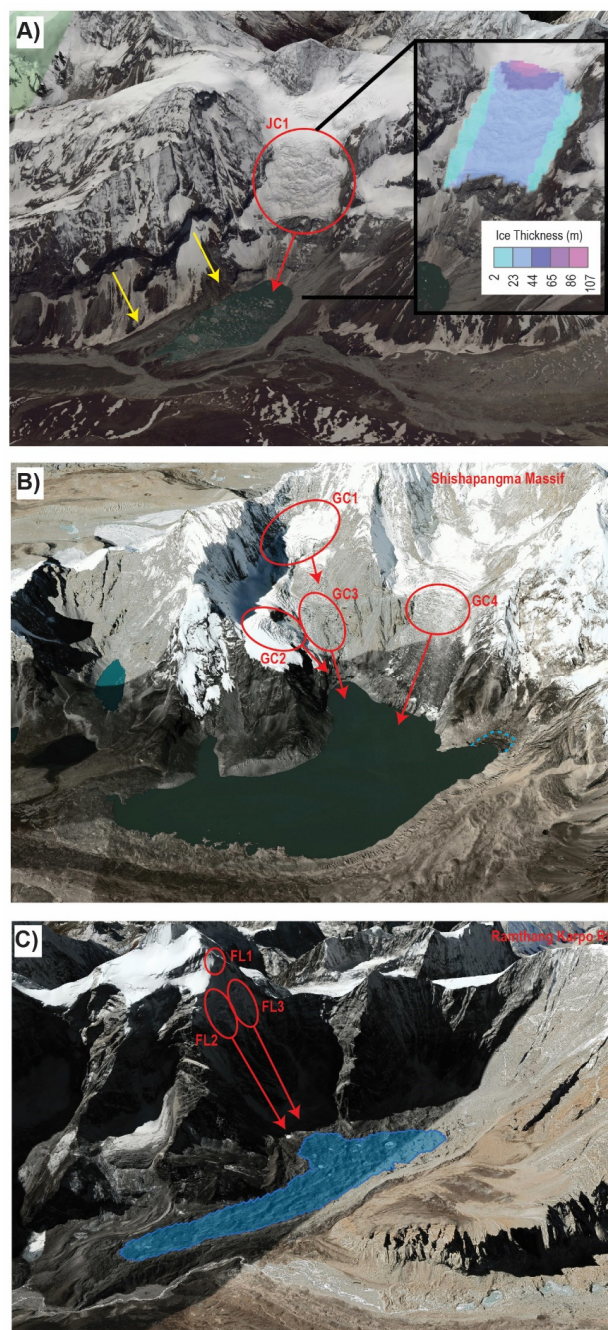


Figure 5: Primary ice avalanche starting zones (in red) threatening the assessed glacial lakes. A) Jialongco: The inset shows the GLABTOP modelled ice thickness of the main avalanche source area, and yellow lines indicate the steep lateral moraine walls also threatening the lake. B) Galongco: Future minimal expansion of the lake shown by the blue dashed line. C) Projected New Lake: GLABTOP modelled future maximum lake extent in blue. Background imagery from © Google Earth.



Table 4: Measured and modelled dimensions of primary ice avalanche starting zones (see Fig. 1) threatening Jialongco (JC), Galongco (GC) and the Future Lake (FL). Mean ice thickness and resulting ice volume is based on GLABTOP.

	Mean slope (°)	Mean ice thickness (m)	Ice area (m ²)	Ice volume (10 ⁶ m ³)	Angle of reach (tan ⁻¹)
JC1	36	34	589,126	19.9	0.48
GC1	35	45	482,144	21.8	0.37
GC2	30	39	229,686	8.9	0.42
GC3	26	43	352,274	15.0	0.41
GC4	25	53	236,424	12.6	0.37
FL1	42	8	12,119	0.1	0.56
FL2	47	24	48,809	1.1	0.49
FL3	52	27	27,305	0.7	0.51

4.3 GLOF impact and exposure

We identify from Open Street Map and Google Earth imagery, the buildings in Nyalam exposed to different GLOF intensity levels according to simulated flood flow heights (after Pozzi *et al.*, 2005). While classification schemes vary across countries, land areas potentially affected by high flood or debris flow intensities (calculated on the basis of flow heights and/or flow velocities), are typically considered as high hazard zones even for low probability events (GAPHAZ, 2017). In Nyalam, lower flow heights associated with an outburst from Jialongco result in lower levels of exposure compared to simulated events from Galongco or the potential future lake (Fig. 6). The majority of buildings in Nyalam are located high above the river channel, where they are safe even in the event of a worst-case outburst scenario. However, it is clear that the rapid expansion of infrastructure along the river banks north of the main settlement over the past several years has significantly increased the built area exposed to potential GLOF events, with many new buildings located in the high intensity flood zone. Overall, levels of exposure are comparable for simulated outbursts from both Galongco and the potential future lake, with both events likely to disrupt the main national road and bridges linking to the town.

Downstream from Nyalam in the reach to the border with Nepal there are few buildings located along the river bank, and the main threat is to a 7.5 km stretch of the transnational highway (Fig. 4), of which the proportion affected by high intensity flood levels is 74% and 96%, for modelled outbursts from Jialongco and Galongco respectively (up to 98% for the potential future lake scenario). While we did not simulate beyond the border owing to the limited coverage of the required high resolution Pleiades DEM, previous events (e.g., Cook *et al.*, 2018; Wang *et al.*, 2018), and assessment studies (Khanal *et al.*, 2015a; Shrestha *et al.*, 2010) have highlighted the significant risk to Nepalese communities, hydropower stations, and other infrastructure located along the banks of the Bhotekoshi river.

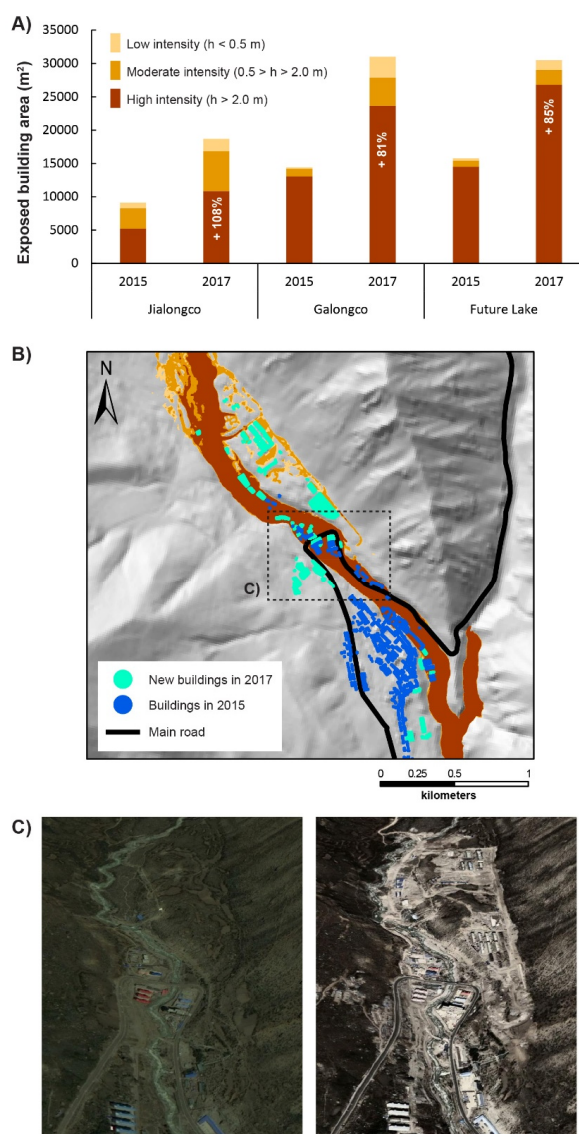
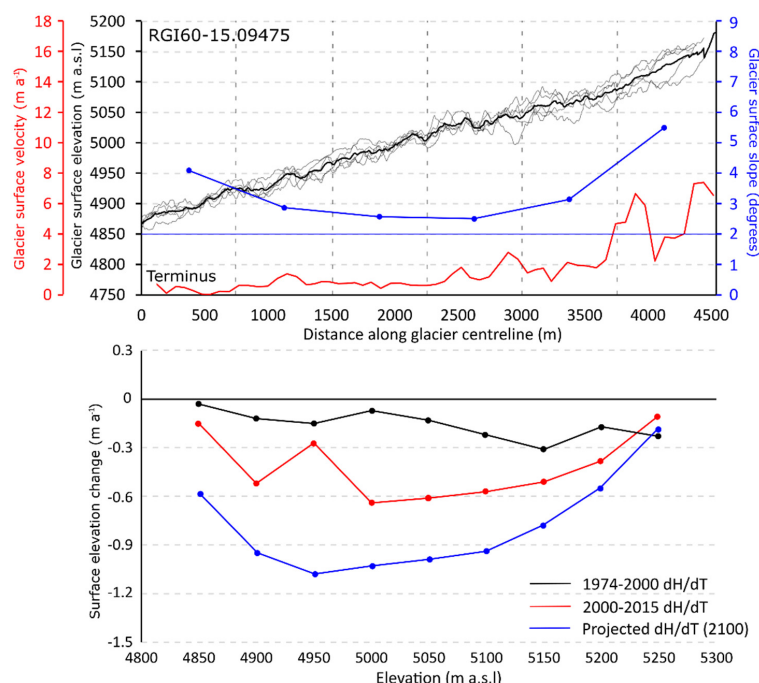


Figure 6: A) Built area in Nyalam exposed to modelled GLOF intensity levels for the three assessed lakes, showing the effect of rapid infrastructural development between 2015 and 2017. The percentage indicates the increase in built area within the high intensity zone. B) Modelled intensities for the Galongco outburst scenarios showing the recent expansion of infrastructure, as seen in © Google Earth imagery (C) from June 2015 (left) and October 2017 (right).

4.4 Trajectory of future lake development

The thinning of glacier RGI60-15.09475 over at least the last four decades has caused the development of a glacier surface that is well suited for supraglacial lake development (Fig. 8). The central 2.5 km of the glacier's ablation zone, where supraglacial ponds are already forming, is effectively stagnant, very gently sloping and has become heavily pitted due to differential ablation in response to spatially variable debris thickness. These conditions will enable the further expansion of the supraglacial pond network, which is unlikely to drain quickly.



405

Figure 7: (A) Surface topography, slope and velocity regime of glacier RGI60-15.09475 in 2017/18. Widespread meltwater ponding is expected once glacier surface slope declines to $\sim 2^\circ$ and little flow is evident to allow for crevasse formation and meltwater drainage. (B) Surface elevation change over the glacier from DEM differencing over the period 1974-2000 and 2000-2015 and the rate of elevation change projected to occur by 2100 (Scenario 1). The same gradient of thinning is assumed to occur by 2056 and be replicated again by 2097 in Scenario 2.

410

The extrapolation of thinning measured over the last four decades over glacier RGI60-15.09475 suggests that a large portion of the glaciers surface will soon sit below an elevation where supraglacial meltwater would normally drain from the glacier surface, allowing for the development of a supraglacial lake. Under scenario 1 (1974-2015 thinning replicated by 2100), 0.6 km² of the glaciers surface will be below the hydrological base level of the glacier by 2100 (Fig. 8). The majority of this area will be located within 1 km of the glacier's terminal moraine, although some small areas further up-glacier will also sit below the hydrological base level by 2100 due to the glacier's inverse ablation gradient (Fig. 7). Under scenario 2 (1974-2015 thinning replicated by 2056, 2097), up to 1.33 km² of the surface of glacier RGI60-15.09475 will sit below the hydrological base level of the glacier by 2100. In addition to the large area proximal to the terminus of the glacier which will sit below the hydrological base level, a large portion of the glacier surface above the overdeepening identified by GlabTop will also have become susceptible to supraglacial lake expansion (Fig. 8c).

420

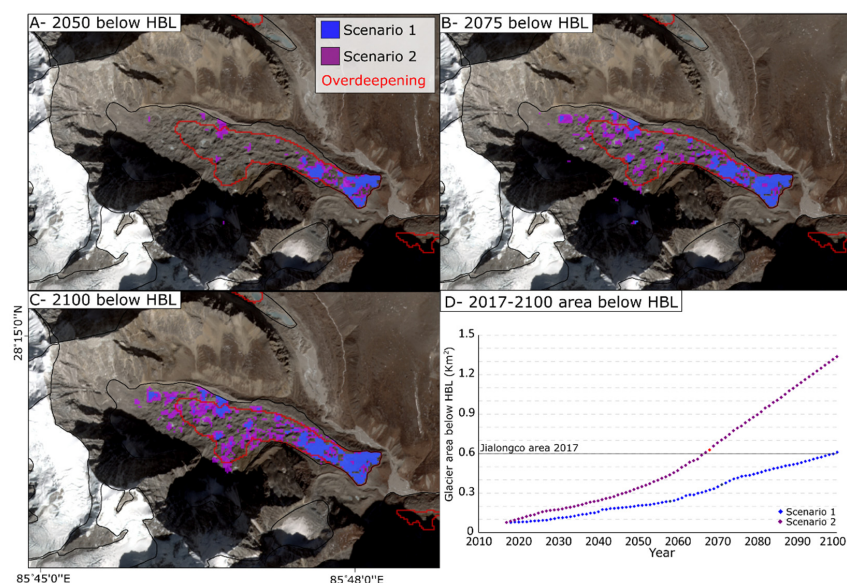


Figure 8: Meltwater ponding (if elevation < the hydrological base level of the glacier) by 2050 (A), 2075 (B) and 2100 (C) under different scenarios of thinning for glacier RGI60-15.09475. The full timeline of supraglacial lake area expansion is shown in (D).

Projected thinning exceeds the ice thickness estimated by GlabTop in current ablation hotspots, most notably towards the terminus of the glacier, where the future ice surface elevation is similar to the simulated bedrock elevation by 2070 under scenario 1 and 2045 under scenario 2. Extrapolated thinning does not match the estimated ice thickness over the majority of the area of the proposed overdeepening further up glacier, where GlabTop suggests ice could be up to 230 m thick.

5 Discussion

The results from this study demonstrate how, on the primary basis of remotely sensed datasets and GIS tools, GLOF risk management planning at the basin-scale can be expanded to consider new threats that may develop in the future. In doing so, this study has taken established approaches for lake susceptibility assessment (GAPHAZ 2017) and outburst modelling (Westoby *et al.*, 2014) and applied these approaches for the first time to consider also an outburst scenario from a potential future lake. To the extent possible, the assessment was based on freely available data and imagery. However, in steep, complex topography such data can have limitations, and a high-resolution DEM derived from Pleiades imagery was required to achieve accurate GLOF modelling results for Poiqu River basin. While not intended to substitute the type of comprehensive model and field-based hazard mapping that needs to support decision-making (e.g., Frey *et al.*, 2018), the results from this study provide an intermediary step for risk management planning. Using the tools and approaches demonstrated here, authorities can effectively bridge the knowledge gap between the known existing threats to which they must immediately respond, and those potential, yet poorly constrained threats that are anticipated emerge in the future.

For the Poiqu basin, these results come at an opportune time, given that local authorities over the past year appear to have initiated major engineering work at Jialongco (Fig. 9). In principle, the focus of authorities on Jialongco is supported by the results of this study, which indicate that the lake poses the greatest immediate threat to the village of Nyalam, and, under a worst-case scenario, will lead to significant flood heights and velocities downstream in Nepal. While less likely, a large



outburst from Galongco would result in a higher intensity flood event, although full drainage of the lake volume is not considered feasible. In fact, despite its rapid expansion over recent years (Wang *et al.*, 2015b; Zhang *et al.*, 2019), the maximum potential flood volume of Galongco, as limited by the dam geometry and potential height of the moraine breach, would likely not have changed. Nonetheless, our simulations reveal a potential peak discharge under a worst-case scenario that is more than 10 times larger than indicated by previous modeling (Shrestha *et al.*, 2010), suggesting that previously estimated potential property losses of up to US\$197 million in downstream communities of Nepal are a lower limit to what could feasibly occur.

Despite the threat the lake poses, the focus at Jialongco on hard engineering strategies to reduce GLOF risk could prove both costly and inefficient, if not complimented by a more comprehensive and forward looking strategy. Although the overall strategy of authorities is not clear, the recent removal of much of the frontal moraine and apparent enhancement of the outlet channel has had only a minimal effect on the overall lake size. Conversely, the resulting removal of the dam freeboard now leaves the lake more susceptible to an overtopping wave, caused by a potential ice avalanche or instability of the lateral moraine wall. In general, increasing exposure of people and assets is seen as a main driver of disaster risk in mountain regions (Hock *et al.*, 2019), and this is clearly evidenced through the rapid increase in built infrastructure upstream of Nyalam over a two-year period, directly within the high intensity zone of potential GLOF paths (Fig. 6). Significant and permanent lowering of the water level in Jialongco would reduce the threat to these buildings from an outburst from this lake, but similar action would need to be repeated at Galongco and as new lakes emerge in the future, in order to minimise potentially larger, albeit, lower probability threats. We would therefore argue that a focus on early warning systems coupled with effective land use zoning and capacity building programs (e.g., Huggel *et al.*, 2020), would provide a more effective, ecologically responsible, and forward looking response strategy, reducing the risk not only from an outburst from Jialongco, but also future-proofing against large outburst scenarios from Galongco or potential new lakes that may develop in the future.

While GlabTop and other similar modelling approaches (see Farinotti *et al.*, 2019a) have been widely used to anticipate future glacial lake locations and assess related risks and opportunities (e.g., Farinotti *et al.*, 2019b; Haeberli *et al.*, 2016a; Magnin *et al.*, 2015), large uncertainties remain as to if and when specific overdeepenings will transition into lakes. In this study, we have focussed on a very large overdeepening positioned beneath a flat, heavily debris covered glacier tongue – a classic geomorphological setting in which large proglacial lakes typically develop (Benn *et al.*, 2012; Haritashya *et al.*, 2018), and analogous to the setting of Galongco. Coupled with the fact that conditions at the surface of the glacier have already allowed supraglacial lakes to form in the ablation zone of the glacier, there can be a high degree of confidence that a future proglacial lake will develop in this location, trapped behind the prominent terminal moraine. The extrapolation of measured thinning rates over the glacier (Fig. 7) allowed for the estimation of when a glacial lake may begin to develop within the boundary of the overdeepening beneath the glacier (Fig. 8). If the acceleration in thinning of the glacier which has occurred over the last four decades is replicated by 2100 (Scenario 1), or over an equivalent time period to that examined by King *et al.* (2019) (1974-2015- Scenario 2), 0.6-1.3 km² of the glaciers surface will sit below the hydrological base level of the glacier and therefore will likely host supraglacial meltwater. Under scenario 1, supraglacial lake area equivalent to the current area of Jialongco will be replicated on glacier RGI60-15.09475 by 2100, and by ~2067 under scenario 2 (Fig. 8). These two scenarios of thinning may still represent a conservatively slower trajectory of lake development on this glacier. Both the development of extensive supraglacial ponds and ice cliff networks and the transition of a supraglacial lake to a full depth proglacial lake can increase the overall thinning rate in the ablation zone of debris-covered glaciers (King *et al.*, 2020; Mölg *et al.*, 2020; Thompson *et al.*, 2016). Our simple extrapolation of current thinning rates and patterns does not account for the initiation or expansion of these



ablative processes. Therefore, we would rather expect greater thinning than our results predict in the lowermost ~1.5 km of the glacier over coming decades once a substantial amount of meltwater has ponded at the glaciers surface.

490

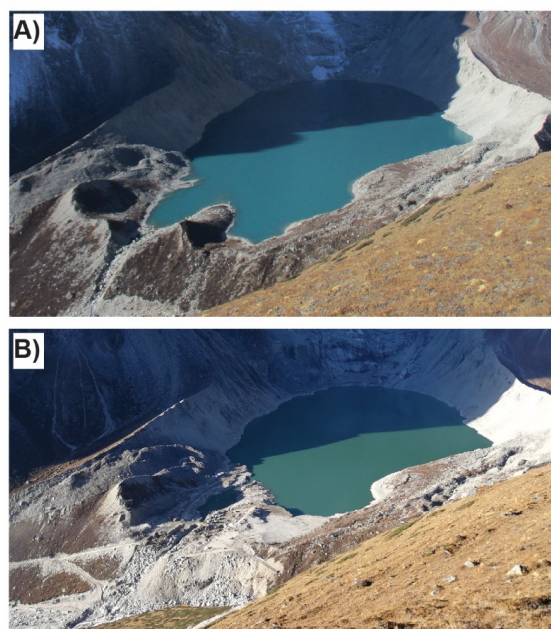


Figure 9: Images taken of Jialongco in A) October 2018, and B) October 2020, clearly showing the engineering work that has been undertaken in the outlet area of the lake. Photos: T. Bolch (A) and G. Zhang (B).

495 In general, the results from this study suggest that hazard mapping and land use planning that accounts for worst-case outburst threats from Jialongco, and particularly Galongco, would largely remain valid for the future lake scenario, given only small differences in the potential built area affected (Fig. 6). In other words, despite uncertainties in the potential speed of future lake development, the opportunity cost of extending hazard zones and related planning to include areas potentially affected under future scenarios is minimal, particularly when considering the protection of critical infrastructure and services. Likewise
 500 for early warning, simulations show that warning times could be reduced by up to 20 minutes for downstream communities in Nepal, under a future outburst scenario. Hence, in order to ensure warning systems and response strategies remain robust over the longer-term, it is recommended that authorities consider such future scenarios in the design phase, under the philosophy of preparing for the worst, while hoping for the best. Particularly in complex transboundary regions requiring communication and collaboration between countries, minutes lost or gained can be critical for effective early warning and evacuation.

505 5 Conclusions

The Poiqu basin in the central Himalaya has been well established as a hotspot from which transboundary GLOF threats can originate. In the current study, we have focused on two lakes that directly threaten the Tibetan town of Nyalam and areas downstream, comparing the likelihood, potential magnitude, and impacts of large outburst events from these lakes. In addition a future scenario has been modelled, whereby an outburst was simulated for a potential new lake, anticipated to form upstream



510 of Jialongco. For all lakes, worst-case scenarios were simulated, assuming release of the full potential flood volume of the lake as defined by the maximum breach height of the moraines. The study has recognised that:

- Jialongco, although smaller in size, poses the greatest current threat to Nyalam and downstream communities, owing to the high potential for an ice avalanche to trigger an outburst, feasibly leading to release of the full potential flood volume. Even though engineering work has started the threat persists as the lake volume remains large and the reduced dam freeboard now leaves the lake more susceptible to an overtopping wave.
- An ice avalanche on its own is considered unlikely to initiate a large outburst from Galongco, although a low-probability/high impact event involving a catastrophic rock/ice avalanche into the lake should be considered as a realistic scenario, particularly given the seismic activity in the region.
- A future scenario, involving the anticipated new lake would lead to flow depths and velocities in Nyalam that exceed either of the current lakes, and the peak wave would reach the border with Nepal up to 20 minutes faster than for the current lakes.
- While previous studies have focused on rapid lake expansion in the region, for the town of Nyalam, it is rather the expansion of infrastructure directly within the high intensity flood zone of both current and future lakes that has significantly increased GLOF risk levels.

On the basis of these findings, a comprehensive and forward-looking approach to disaster risk reduction is called for, combining early warning systems with effective land use zoning and capacity building programs. Hard engineering strategies that address only the hazard source are a socially and environmentally less desirable option, as such strategies do nothing to address underlying risk drivers of exposure and vulnerability, and are likely unsustainable in the face of ongoing environmental changes.



535 **Author contribution**

SA and AS designed the study and undertook the GLOF modelling, and hazard assessment. OK performed the modelling of future lake development. AB produced the high resolution Pleiades DEM. SA, OK, TB, and GZ provided insights from field visits. All authors contributed to the drafting of the manuscript.

540 **Acknowledgement**

This work was supported by the Swiss National Science Foundation (IZLCZ2_169979/1). The work further benefited from support of the Strategic Priority Research Program of the Chinese Academy of Sciences (XDA20060201).

545 **Competing interests**

The authors declare that they have no conflict of interest.



References

- Allen SK, Linsbauer A, Randhawa SS, Huggel C, Rana P, Kumari A. 2016. Glacial lake outburst flood risk in Himachal Pradesh, India: an integrative and anticipatory approach considering current and future threats. *Natural Hazards*. Springer Netherlands **84**(3): 1741–1763. DOI: 10.1007/s11069-016-2511-x.
- Allen SK, Zhang G, Wang W, Yao T, Bolch T. 2019. Potentially dangerous glacial lakes across the Tibetan Plateau revealed using a large-scale automated assessment approach. *Science Bulletin*. Elsevier B.V. **64**(7): 435–445. DOI: 10.1016/j.scib.2019.03.011.
- Benn DI, Bolch T, Hands K, Gulley J, Luckman A, Nicholson LI, Quincey D, Thompson S, Toumi R, Wiseman S. 2012. Response of debris-covered glaciers in the Mount Everest region to recent warming, and implications for outburst flood hazards. *Earth Science Reviews* **114**: 156–174.
- Bhattacharya A, Bolch T, Mukherjee K, King O, Menounos B, Kapitsa V, Neckel N, Yang W, Yao T. 2021. High Mountain Asian glacier response to climate revealed by multi-temporal satellite observations since the 1960s. *Nature Communications* in review.
- Bolch T, Shea JM, Liu S, Azam FM, Gao Y, Gruber S, Immerzeel WW, Kulkarni A, Li H, Tahir AA, Zhang G, Zhang Y. 2019. Status and Change of the Cryosphere in the Extended Hindu Kush Himalaya Region. In: P. W, A. M, A. M and A. S (eds) *The Hindu Kush Himalaya Assessment*. Springer International Publishing: Cham, 209–255. DOI: 10.1007/978-3-319-92288-1_7.
- Carrivick JL, Tweed FS. 2016. A global assessment of the societal impacts of glacier outburst floods. *Global and Planetary Change*. Elsevier B.V. **144**: 1–16. DOI: 10.1016/j.gloplacha.2016.07.001.
- Chen NS, Hu GS, Deng W, Khanal N, Zhu YH, Han D. 2013. On the water hazards in the trans-boundary Kosi River basin. *Natural Hazards and Earth System Science* **13**(3): 795–808. DOI: 10.5194/nhess-13-795-2013.
- Clague JJ, Evans SG. 2000. A review of catastrophic drainage of moraine-dammed lakes in British Columbia. *Quaternary Science Reviews* **19**: 1763–1783.
- Cook KL, Andermann C, Gimbert F, Adhikari BR, Hovius N. 2018. Glacial lake outburst floods as drivers of fluvial erosion in the Himalaya. *Science (New York, N.Y.)*. American Association for the Advancement of Science **362**(6410): 53–57. DOI: 10.1126/science.aat4981.
- Cook SJ, Quincey DJ. 2015. Estimating the volume of Alpine glacial lakes. *Earth Surface Dynamics* **3**(4): 559–575. DOI: 10.5194/esurf-3-559-2015.
- Emmer A, Cochachin A. 2013. The causes and mechanisms of moraine-dammed lake failures in the Cordillera Blanca, North American Cordillera, and Himalayas. *AUC Geographica* **48**: 5–15.
- Emmer A, Harrison S, Mergili M, Allen S, Frey H, Huggel C. 2020. 70 years of lake evolution and glacial lake outburst floods in the Cordillera Blanca (Peru) and implications for the future. *Geomorphology*. Elsevier B.V. **365**: 107178. DOI: 10.1016/j.geomorph.2020.107178.
- Farinotti D, Huss M, Fürst JJ, Landmann J, Machguth H, Maussion F, Pandit A. 2019a. A consensus estimate for the ice thickness distribution of all glaciers on Earth. *Nature Geoscience*. Nature Publishing Group **12**(3): 168–173. DOI: 10.1038/s41561-019-0300-3.
- Farinotti D, Round V, Huss M, Compagno L, Zekollari H. 2019b. Large hydropower and water-storage potential in future glacier-free basins. *Nature*. Springer US **575**(7782): 341–344. DOI: 10.1038/s41586-019-1740-z.
- Frey H, Huggel C, Chisolm RE, Baer P, Mcardell BW, Cochachin A, Portocarrero. 2018. Multi-source glacial lake outburst flood hazard assessment and mapping for Huaraz, Cordillera Blanca, Peru. . DOI: 10.3389/feart.2018.00210.



- Frey H, Haeberli W, Linsbauer A, Huggel C, Paul F. 2010. A multi-level strategy for anticipating future glacier lake formation and associated hazard potentials. *Natural Hazards and Earth System Sciences* **10**: 339–352.
- 590 Froehlich DC. 1995. Peak Outflow from Breached Embankment Dam. *Journal of Water Resources Planning and Management*. Publ by ASCE **121**(1): 90–97. DOI: 10.1061/(ASCE)0733-9496(1995)121:1(90).
- Fujita K, Sakai A, Takenaka S, Nuimura T, Surazakov AB, Sawagaki T, Yamanokuchi T. 2013. Potential flood volume of Himalayan glacial lakes. *Natural Hazards and Earth System Science* **13**(7): 1827–1839. DOI: 10.5194/nhess-13-1827-2013.
- 595 Furian W, Loibl D, Schneider C. 2021. Future glacial lakes in High Mountain Asia: an inventory and assessment of hazard potential from surrounding slopes. *Journal of Glaciology*. Cambridge University Press (CUP) 1–18. DOI: 10.1017/jog.2021.18.
- GAPHAZ. 2017. *Assessment of Glacier and Permafrost Hazards in Mountain Regions: Technical Guidance Document*. Standing Group on Glacier and Permafrost Hazards in Mountains (GAPHAZ) of the International Association of Cryospheric Sciences (IACS) and the International Permafrost Association (IPA). Zurich, Switzerland /
- 600 Lima, Peru.
- Gardelle J, Arnaud Y, Berthier E. 2011. Contrasted evolution of glacial lakes along the Hindu Kush Himalaya mountain range between 1990 and 2009. *Global and Planetary Change* **75**: 47–55.
- Haeberli W, Buetler M, Huggel C, Lehmann Friedli T, Schaub Y, Schleiss AJ. 2016a. New lakes in deglaciating high- mountain regions – opportunities and risks. *Climatic Change* **139**: 201–214.
- 605 Haeberli W, Schaub Y, Huggel C. 2016b. Increasing risks related to landslides from degrading permafrost into new lakes in de-glaciating mountain ranges. *Geomorphology* doi: 10.1016/j.geomorph.2016.02.009.
- Haritashya UK, Kargel JS, Shugar DH, Leonard GJ, Strattman K, Watson CS, Shean D, Harrison S, Mandli KT, Regmi D. 2018. Evolution and controls of large glacial lakes in the Nepal Himalaya. *Remote Sensing* **10**(5): 1–31. DOI: 10.3390/rs10050798.
- 610 Harrison S, Kargel JS, Huggel C, Reynolds J, Shugar DH, Betts RA, Emmer A, Glasser N, Haritashya UK, Klimeš J, Reinhardt L, Schaub Y, Wiltshire A, Regmi D, Vilímek V. 2018. Climate change and the global pattern of moraine-dammed glacial lake outburst floods. *The Cryosphere* **12**(4): 1195–1209. DOI: 10.5194/tc-12-1195-2018.
- 615 Hock R, Rasul G, Adler C, Cáceres B, Gruber S, Hirabayashi Y, Jackson M, Kääb A, Kang S, Kutuzov S, Milner A, Molau U, Morin S, Orlove B, Steltzer H. 2019. *High Mountain Areas*. In: *IPCC Special Report on the Ocean and Cryosphere in a Changing Climate* [H.-O. Pörtner, D.C. Roberts, V. Masson-Delmotte, P. Zhai, M. Tignor, E. Poloczanska, K. Mintenbeck, A. Alegría, M. Nicolai, A. Okem, J. Petzold, B. Rama, N.M.].
- Huggel C, Cochachin A, Drenkhan F, Fluixá-Sanmartín J, Frey H, García Hernández J, Jurt C, Muñoz R, Price K, Vicuña L. 2020. Glacier Lake 513, Peru: lessons for early warning service development. *WMO Bulletin* **69**(1): 45–52.
- 620 Huggel C, Haeberli W, Kääb A, Bieri D, Richardson S. 2004. An assessment procedure for glacial hazards in the Swiss Alps. *Canadian Geotechnical Journal* **41**: 1068–1083.
- Kääb A, Jacquemart M, Gilbert A, Leinss S, Girod L, Huggel C, Falaschi D, Ugalde F, Petrakov D, Chernomorets S, Dokukin M, Paul F, Gascoin S, Berthier E, Kargel JS. 2021. Sudden large-volume detachments of low-angle mountain glaciers – more frequent than thought? *The Cryosphere* **15**(4): 1751–1785. DOI: 10.5194/tc-15-1751-2021.
- 625 Khanal NR, Hu J-M, Mool P. 2015a. Glacial Lake Outburst Flood Risk in the Poiqu/Bhote Koshi/Sun Koshi River



- Basin in the Central Himalayas. *Mountain Research and Development* **35**: 351–364.
- 630 Khanal NR, Mool PK, Shrestha AB, Rasul G, Ghimire PK, Shrestha RB, Joshi SP. 2015b. A comprehensive approach and methods for glacial lake outburst flood risk assessment, with examples from Nepal and the transboundary area. *International Journal of Water Resources Development* **31**: 219–237.
- King O, Bhattacharya A, Bhambri R, Bolch T. 2019. Glacial lakes exacerbate Himalayan glacier mass loss. *Scientific Reports*. Nature Research **9**(1). DOI: 10.1038/s41598-019-53733-x.
- 635 King O, Bhattacharya A, Ghuffar S, Tait A, Guilford S, Elmore AC, Bolch T. 2020. Six Decades of Glacier Mass Changes around Mt. Everest Are Revealed by Historical and Contemporary Images. *One Earth*. Cell Press **3**(5): 608–620. DOI: 10.1016/j.oneear.2020.10.019.
- King O, Dehecq A, Quincey D, Carrivick J. 2018. Contrasting geometric and dynamic evolution of lake and land-terminating glaciers in the central Himalaya. *Global and Planetary Change*. Elsevier B.V. **167**: 46–60. DOI: 10.1016/j.gloplacha.2018.05.006.
- 640 Klimeš J, Novotný J, Novotná I, de Urries BJ, Vilímek V, Emmer A, Strozzi T, Kusák M, Rapre AC, Hartvich F, Frey H. 2016. Landslides in moraines as triggers of glacial lake outburst floods: example from Palcacocha Lake (Cordillera Blanca, Peru). *Landslides*. Springer Verlag **13**(6): 1461–1477. DOI: 10.1007/s10346-016-0724-4.
- Korup O, Tweed F. 2007. Ice, moraine, and landslide dams in mountainous terrain. *Quaternary Science Reviews* **26**: 3406–3422.
- 645 Kraaijenbrink PDA, Bierkens MFP, Lutz AF, Immerzeel WW. 2017. Impact of a global temperature rise of 1.5 degrees Celsius on Asia's glaciers. *Nature Publishing Group* **549**: 5–7. DOI: 10.1038/nature23878.
- Linsbauer A, Frey H, Haeberli W, Machguth H, Azam MF, Allen S. 2016. Modelling glacier-bed overdeepenings and possible future lakes for the glaciers in the Himalaya–Karakoram region. *Annals of Glaciology* **57**: 119–130.
- 650 Linsbauer A, Paul F, Haeberli W. 2012. Modeling glacier thickness distribution and bed topography over entire mountain ranges with GlabTop: application of a fast and robust approach. *Journal of Geophysical Research* **117**: doi: 10.1029/2011JF002313.
- Linsbauer A, Paul F, Machguth H, Haeberli W. 2013. Comparing three different methods to model scenarios of future glacier change in the Swiss Alps. *Annals of Glaciology* **54**: 241–253.
- 655 Liu J-J, Tang C, Cheng Z-L. 2013. The Two Main Mechanisms of Glacier Lake Outburst Flood in Tibet, China. *J. Mt. Sci* **10**(2): 239–248. DOI: 10.1007/s11629-013-2517-8.
- Lliboutry L, Morales AB, Pautre A, Schneider B. 1977. Glaciological problems set by the control of dangerous lakes in Cordillera Blanca, Peru. I. Historic failure of morainic dams, their causes and prevention. *Journal of Glaciology* **18**: 239–254.
- 660 Magnin F, Haeberli W, Linsbauer A, Deline P, Ravanel L. 2020. Estimating glacier-bed overdeepenings as possible sites of future lakes in the de-glaciating Mont Blanc massif (Western European Alps). *Geomorphology*. Elsevier B.V. **350**. DOI: 10.1016/j.geomorph.2019.106913.
- Magnin F, Krautblatter M, Deline P, Ravanel L, Malet E, Bevington A. 2015. Determination of warm, sensitive permafrost areas in near-vertical rockwalls and evaluation of distributed models by electrical resistivity tomography. *Journal of Geophysical Research-Earth Surface* **120**: 745–762.
- 665 Maurer JM, Schaefer JM, Rupper S, Corley A. 2019. Acceleration of ice loss across the Himalayas over the past 40 years. *Science Advances*. American Association for the Advancement of Science **5**(6): eaav7266. DOI: 10.1126/sciadv.aav7266.
- Mölg N, Ferguson J, Bolch T, Vieli A. 2020. On the influence of debris cover on glacier morphology: How high-relief



- 670 structures evolve from smooth surfaces. *Geomorphology*. Elsevier B.V. **357**: 107092. DOI:
 10.1016/j.geomorph.2020.107092.
- Nie Y, Liu Q, Wang J, Zhang Y, Sheng Y, Liu S. 2018. An inventory of historical glacial lake outburst floods in the
 Himalayas based on remote sensing observations and geomorphological analysis. *Geomorphology*. Elsevier
 B.V. **308**: 91–106. DOI: 10.1016/j.geomorph.2018.02.002.
- 675 Nie Y, Sheng Y, Liu Q, Liu L, Liu S, Zhang Y, Song C. 2017. A regional-scale assessment of Himalayan glacial lake
 changes using satellite observations from 1990 to 2015. *Remote Sensing of Environment*. Elsevier Inc. **189**: 1–
 13. DOI: 10.1016/j.rse.2016.11.008.
- Pozzi A, Stössel F, Zimmermann M. 2005. *Vademecum hazard maps and related instruments : the Swiss system and
 its application abroad : capitalisation of experiences*. Swiss Agency for Development and Cooperation (SDC),
 680 Bern.
- Pronk JB, Bolch T, King O, Wouters B, Benn DI. 2021. Proglacial Lakes Elevate Glacier Surface Velocities in the
 Himalayan Region. *The Cryosphere Discussions* in review. DOI: 10.5194/tc-2021-90.
- Quincey DJ, Richardson SD, Luckman A, Lucas RM, Reynolds JM, Hambrey MJ, Glasser NF. 2007. Early recognition
 of glacial lake hazards in the Himalaya using remote sensing datasets. *Global and Planetary Change* **56**: 137–
 685 152.
- Ren Y-Y, Ren G-Y, Sun X-B, Shrestha AB, You Q-L, Zhan Y-J, Rajbhandari R, Zhang P-F, Wen K-M. 2017. Observed
 changes in surface air temperature and precipitation in the Hindu Kush Himalayan region over the last 100-
 plus years. *Advances in Climate Change Research* **8**(3): 148–156. DOI: 10.1016/j.accr.2017.08.001.
- Richardson SD, Reynolds JM. 2000. An overview of glacial hazards in the Himalayas. *Quaternary International* **65/66**:
 690 31–47.
- Romstad B, Harbitz C], Domaas U. 2009. A GIS method for assessment of rock slide tsunami hazard in all Norwegian
 lakes and reservoirs. *Natural Hazards and Earth System Sciences* **9**: 353–364.
- Sanjay J, Krishnan R, Shrestha AB, Rajbhandari R, Ren GY. 2017. Downscaled climate change projections for the
 Hindu Kush Himalayan region using CORDEX South Asia regional climate models. *Advances in Climate
 Change Research*. National Climate Center **8**(3): 185–198. DOI: 10.1016/j.accr.2017.08.003.
- 695 Sattar A, Haritashya UK, Kargel JS, Leonard GJ, Shugar DH, Chase D V. 2021. Modeling Lake Outburst and
 Downstream Hazard Assessment of the Lower Barun Glacial Lake, Nepal Himalaya. *Journal of Hydrology*.
 Elsevier BV **598**: 126208. DOI: 10.1016/j.jhydrol.2021.126208.
- Schaub Y, Huggel C, Cochachin A. 2015. Ice-avalanche scenario elaboration and uncertainty propagation in numerical
 700 simulation of rock-/ice-avalanche-induced impact waves at Mount Hualcán and Lake 513, Peru. *Landslides*
 doi:10.1007/s10346-015-0658-2.
- Schmid M-O, Baral P, Gruber S, Shahi S, Shrestha T, Stumm D, Wester P. 2015. Assessment of permafrost distribution
 maps in the Hindu Kush Himalayan region using rock glaciers mapped in Google Earth. *The Cryosphere* **9**:
 2089–2099.
- 705 Schneider D, Huggel C, Haeberli W, Kaitna R. 2011. Unraveling driving factors for large rock-ice avalanche mobility.
Earth Surface Processes and Landforms **36**: 1948–1966.
- Shedlock KM, Giardini D, Grünthal G, Zhang P. 2000. The GSHAP Global Seismic Hazard Map. *Seismological
 Research Letters*. Seismological Society of America **71**(6): 679–686. DOI: 10.1785/gssrl.71.6.679.
- Shijin W, Shitai J. 2015. Evolution and outburst risk analysis of moraine-dammed lakes in the central Chinese
 710 Himalaya. *Journal of Earth System Science*. Springer India **124**(3): 567–576. DOI: 10.1007/s12040-015-0559-



- 8.
- Shrestha AB, Eriksson M, Mool P, Ghimire P, Mishra B, Khanal NR. 2010. Glacial lake outburst flood risk assessment of Sun Koshi basin, Nepal. *Geomatics, Natural Hazards and Risk*. Taylor & Francis **1**(2): 157–169. DOI: 10.1080/19475701003668968.
- 715 Shugar DH, Burr A, Haritashya UK, Kargel JS, Watson CS, Kennedy MC, Bevington AR, Betts RA, Harrison S, Strattman K. 2020. Rapid worldwide growth of glacial lakes since 1990. *Nature Climate Change*. Springer US **10**(10): 939–945. DOI: 10.1038/s41558-020-0855-4.
- Thompson S, Benn DI, Mertes J, Luckman A. 2016. Stagnation and mass loss on a Himalayan debris-covered glacier: Processes, patterns and rates. *Journal of Glaciology*. International Glaciology Society **62**(233): 467–485. DOI: 10.1017/jog.2016.37.
- 720 Veh G, Korup O, von Specht S, Roessner S, Walz A. 2019. Unchanged frequency of moraine-dammed glacial lake outburst floods in the Himalaya. *Nature Climate Change*. Nature Publishing Group, 379–383. DOI: 10.1038/s41558-019-0437-5.
- Wang S, Dahe Q, Xiao C. 2015a. Moraine-dammed lake distribution and outburst flood risk in the Chinese Himalaya. *Journal of Glaciology* **61**: 115–126.
- 725 Wang S, Zhou L. 2017. Glacial Lake Outburst Flood Disasters and Integrated Risk Management in China. *International Journal of Disaster Risk Science* **8**. DOI: 10.1007/s13753-017-0152-7.
- Wang W, Gao Y, Iribarren Anaconda P, Lei Y, Xiang Y, Zhang G, Li S, Lu A. 2018. Integrated hazard assessment of Cirenmaco glacial lake in Zhangzangbo valley, Central Himalayas. *Geomorphology*
 http://dx.doi.org/10.1016/j.geomorph.2015.08.013.
- 730 Wang W, Xiang Y, Gao Y, Lu A, Yao T. 2015b. Rapid expansion of glacial lakes caused by climate and glacier retreat in the Central Himalayas. *Hydrological Processes*. John Wiley & Sons, Ltd **29**(6): 859–874. DOI: 10.1002/hyp.10199.
- Westoby MJ, Glasser NF, Brasington J, Hambrey MJ, Quincey DJ, Reynolds JM. 2014. Modelling outburst floods from moraine-dammed glacial lakes. *Earth-Science Reviews* **134**: 137–159. DOI: http://dx.doi.org/10.1016/j.earscirev.2014.03.009.
- 735 Worni R, Stoffel M, Huggel C, Volz C, Casteller A, Luckman B. 2012. Analysis and dynamic modeling of a moraine failure and glacier lake outburst flood at Ventisquero Negro, Patagonian Andes (Argentina). *Journal of Hydrology* **444–445**: 134–145.
- 740 Xu D. 1988. Characteristics of debris flow caused by outburst of glacial lake in Boqu river, Xizang, China, 1981. *GeoJournal*. Kluwer Academic Publishers **17**(4): 569–580. DOI: 10.1007/BF00209443.
- Zemp M, Huss M, Thibert E, Eckert N, McNabb R, Huber J, Barandun M, Machguth H, Nussbaumer SU, Gärtner-Roer I, Thomson L, Paul F, Maussion F, Kutuzov S, Cogley JG. 2019. Global glacier mass changes and their contributions to sea-level rise from 1961 to 2016. *Nature*. Nature Publishing Group, 382–386. DOI: 10.1038/s41586-019-1071-0.
- 745 Zhang G, Bolch T, Allen S, Linsbauer A, Chen W, Wang W. 2019. Glacial lake evolution and glacier–lake interactions in the Poiqu River basin, central Himalaya, 1964–2017. *Journal of Glaciology*. Cambridge University Press 1–19. DOI: 10.1017/jog.2019.13.
- Zhang G, Yao T, Xie H, Wang W, Yang W. 2015. An inventory of glacial lakes in the Third Pole region and their changes in response to global warming. *Global and Planetary Change* **131**: 148–157.
- 750 Zheng G, Allen SK, Bao A, Ballesteros-Cánovas JA, Huss M, Zhang G, Li L, Yuan Y, Jiang L, Yu T, Chen W, Stoffel



- M. 2021a. Increasing risk of glacial lake outburst floods from future Third Pole deglaciation. *Nature Climate Change* <https://doi.org/10.1038/s41558-021-01028-3>.
- 755 Zheng G, Mergili M, Emmer A, Allen S, Bao A, Guo H, Stoffel M. 2021b. The 2020 glacial lake outburst flood at Jinwucuo, Tibet: causes, impacts, and implications for hazard and risk assessment. *The Cryosphere Discussions* 1–28. DOI: 10.5194/tc-2020-379.